

# GPS sidereal filtering: coordinate- and carrier-phase-level strategies

A. E. Ragheb · P. J. Clarke · S. J. Edwards

Received: 27 April 2006 / Accepted: 7 October 2006 / Published online: 21 November 2006  
© Springer-Verlag 2006

**Abstract** Multipath error is considered one of the major errors affecting GPS observations. One can benefit from the repetition of satellite geometry approximately every sidereal day, and apply filtering to help minimize this error. For GPS data at 1 s interval processed using a double-difference strategy, using the day-to-day coordinate or carrier-phase residual autocorrelation determined with a 10-h window leads to the steadiest estimates of the error-repeat lag, although a window as short as 2 h can produce an acceptable value with >97% of the optimal lag's correlation. We conclude that although the lag may vary with time, such variation is marginal and there is little advantage in using a satellite-specific or other time-varying lag in double-difference processing. We filter the GPS data either by stacking a number of days of processed coordinate residuals using the optimum "sidereal" lag (23 h 55 m 54 s), and removing these stacked residuals from the day in question (coordinate space), or by a similar method using double-difference carrier-phase residuals (observational space). Either method results in more consistent and homogeneous set of coordinates throughout the dataset compared with unfiltered processing. Coordinate stacking reduces geometry-related repeating errors (mainly multipath) better than carrier-phase residual stacking, although the latter takes less processing time to achieve final filtered coordinates. Thus, the optimal stacking method will depend on whether coordinate precision or computational time is the over-riding criterion.

**Keywords** GPS · Multipath · Sidereal filter · Autocorrelation · Single epoch positioning

## 1 Introduction

Although most of the errors affecting short-baseline GPS are eliminated or minimized by differencing techniques (e.g., [Leick 2004](#)), multipath error will remain due to the highly site-specific nature of the reflection of GPS signals from nearby surfaces. Accordingly, multipath is often considered the most limiting factor in precise GPS positioning (e.g. [Lau and Mok 1999](#); [Axelrad et al. 1996](#)). Short-term positions will be subject to quasi-periodic errors with characteristic time scales varying from seconds to minutes depending on the satellite-reflector geometry. Long-term position monitoring is also affected: if GPS data are processed in 24-solar-hour batches, as is often the case, multipath error occurring at the satellite geometry repeat interval can alias into periodic errors at annual and semi-annual periods ([Penna and Stewart 2003](#)).

Several techniques are used in the reduction of multipath. At the point of measurement, the use of choke-ring antennas or special architecture receivers with built-in multipath mitigation techniques eliminates much of the code multipath, leaving carrier-phase multipath still dominant, which is a more embedded and harder-to-mitigate source of error ([Filippov et al. 1999](#); [Van Dierendonck and Braaasch 1997](#)). Other recent techniques reduce the multipath error at the post-processing stage, minimizing carrier-phase or code multipath using either wavelet analysis ([Satirapod and Rizos 2005](#)), a Vondrak filter with cross-validation

---

A. E. Ragheb (✉) · P. J. Clarke · S. J. Edwards  
School of Civil Engineering and Geosciences,  
Newcastle University, Cassie Building,  
Newcastle upon Tyne NE1 7RU, UK  
e-mail: Ahmed.Ragheb@ncl.ac.uk

(Zheng et al. 2005), or weighting the data using the observed signal-to-noise ratio (SNR) (Lau and Mok 1999).

Satirapod and Rizos (2005) applied wavelet decomposition to GPS double-difference residuals in order to extract GPS carrier-phase multipath. This multipath signature is then directly removed from GPS carrier-phase observations in subsequent days. By using filters of different cut-off frequencies and comparison with zero baseline double-difference residuals, the optimal level of wavelet filtering is deduced.

In contrast, Zheng et al. 2005 separated carrier-phase signals from noise whenever the noise level is lower than the magnitude of the signal, using a Vondrak filter based on different smoothing factors, with cross validation to determine the optimal smoothing factor. This combination gives a balance between data fitting and smoothing. An improvement in the coordinate RMS of 20–40% was achieved. However, this technique has the disadvantage that at high noise levels, genuine high-frequency signals tend to be filtered out.

The third technique, due to Lau and Mok (1999), uses the SNR determined by the carrier tracking loop in the GPS receiver as a measure of the precision of carrier-phase measurements. SNR weighting is applied to each receiver–satellite pair. This method improves the accuracy even with a small dataset, without any averaging or smoothing of the multipath error. The main disadvantage here is that the SNR is not always present in the RINEX observation file, which makes it inapplicable in many situations.

Due to the nearly exact repetition of GPS satellite geometry in the sky above a site every sidereal day (nominally 23 h 56 m 04 s), multipath error is highly correlated across subsequent days providing the same antenna and reflector environment, and it is possible to apply “side-real filtering” techniques to mitigate this error (Genrich and Bock 1992; Nikolaidis et al. 2001). Essentially, these methods subtract a filter value from the site coordinates at each epoch. The filter at a given epoch is composed from the coordinate residuals to the long-term mean position, at an epoch separated from the application epoch by a whole number of sidereal days (i.e. a multiple of the nominal lag of 86, 164 s).

To improve the precision and robustness of the filter, the residuals may be stacked (averaged) over several sidereal days. Recent investigations based on satellite orbit analysis (Choi et al. 2004) have shown that the actual satellite geometry repeat interval (hereafter, “geometry-repeat lag”) is slightly less than the nominal sidereal period used in the earlier studies. More recently, Larson et al. (2006, <http://www.spot.colorado.edu/~kristine/publications.html>) have discussed the use of

cross correlation within the coordinate residuals to determine the optimal geometry-repeat lag.

Our objectives in this paper are firstly to test the variation in this lag and the possible benefits of using a time-variable lag by the analysis of the periodicity of the coordinate and carrier-phase residuals from single-epoch double-difference positioning, and secondly to establish whether filtering at the coordinate or carrier-phase observation level is the most beneficial. We use data from very short baselines over which clock, orbital and atmospheric errors may be assumed to cancel completely. In deciding the optimal filtering method, we consider not only the improvement in short-term coordinate precision but also the consistency of this improvement, and the processing time necessary to achieve final filtered coordinates. For near-real-time applications, such as landslides, geohazards and monitoring of civil engineering structures, these additional criteria are important.

## 2 Methodology

For GPS data processing, we use an epoch-by-epoch, double-difference, algorithm implemented in the GASP (GPS Ambiguity Search Program) software (Corbett 1994; Al-Haifi 1996). GASP operates in fully kinematic mode, treating each epoch as an entirely independent measurement problem, and conducting a search in ambiguity space for the optimal integer values of the ambiguity parameters using the L1 and L2 phase observables. As each epoch is treated separately, there is no possibility for common parameters to affect the level of multipath error.

GASP processes baselines, either in “kinematic-base” mode in which the coordinates of the “fixed” site are determined by a code pseudorange solution at each epoch, or in “fixed-base” mode in which the coordinates of the “fixed” site are specified a priori. The latter mode of operation was the one used in this paper. Elevation-dependent antenna phase-centre variations are modelled using the US National Geodetic Survey calibration values (<http://www.ngs.noaa.gov/ANTCAL/index.shtml>). For this study, we use International GNSS Service (IGS) final precise orbits (Neilan et al. 1997), although rapid precise orbits could be used with similar accuracy (<http://igs.cb.jpl.nasa.gov/>).

Rather than use an a priori value for the geometry-repeat lag (e.g., the nominal sidereal period, or twice the average satellite orbital period), we search for the optimal lag to use in our filter using the autocorrelation of the station coordinate time-series. The weighted auto-

correlation for any window size of the data can be calculated from

$$AC = 2 \times \frac{\sum_{i=1}^m \frac{\sum_{x=x_0}^z P_{xc} \times (x_t - X_0) \times (x_{t+\tau} - X_0)}{\sum_{x=x_0}^z P_{xc}}}{\sum_{i=1}^m \frac{P_x^t \times (x_t - X_0)^2}{\sum_{x=x_0}^z P_x^t} + \frac{P_x^{t+\tau} \times (x_{t+\tau} - X_0)^2}{\sum_{x=x_0}^z P_x^{t+\tau}}}, \quad (1)$$

where  $AC$  is the autocorrelation,  $\tau$  is a trial value of the “sidereal” lag,  $x_t$  and  $x_{t+\tau}$  are the coordinates at epochs  $t$  and  $t + \tau$ , respectively,  $P_{xc}$  is the combined weight of both epochs,  $P_x^t$  and  $P_x^{t+\tau}$  are the weights of the individual epochs, and  $m$  is the number of processed epochs in the chosen time window.

To determine the optimal lag, we search for the maximum autocorrelation, for a range of trial lags at 1 s intervals within  $\pm 30$  s of the nominal sidereal period. A similar procedure is adopted using the double-difference phase residuals instead of the three components of the site coordinates.

Once we have determined the optimal lag (that with the highest autocorrelation value), we form our filter by stacking residuals at this lag, over one or more days’ observations. For the “coordinate filter”, we use epoch-by-epoch coordinate residuals with respect to the long-term mean coordinate of each site. Filtering is then applied by subtracting these residuals from the processed coordinates at the corresponding epoch of the day in question.

For the “phase filter”, we use double-difference carrier-phase residuals (without ambiguity resolution) with respect to a fully fixed solution in which both ends of the baseline have coordinates fixed to their a priori or long-term mean values. Filtering is then applied by subtracting these stacked phase residuals from the double-difference observations at the corresponding epoch on the day in question, when the latter are formed during processing. Processing then continues as normal, with an ambiguity search followed by a final coordinate estimation. The main criteria used to assess the efficiency of the sidereal filter are the repeatability (precision) of station coordinates over a certain time interval, and the  $F$ -test statistic to test the significance of improvement and level of consistency in the filtered solution.

### 3 Data collection

Four stations on buildings within the Newcastle University campus were chosen, two in a relatively low multipath environment, named *DRMN* and *DRMS*, and two in a higher multipath environment, called *SN02* and *NEWC*. Figure 1 shows the site locations and environment. The latter station is part of the “Active GPS Network” of the Ordnance Survey of Great Britain

(OS). Data were collected at a 1 s observation rate with a  $5^\circ$  elevation mask angle, in order to include low elevation satellites, which generally cause higher multipath error, as is desired to test the robustness of the sidereal filtering for multipath reduction. Table 1 shows the data collection parameters of the primary dataset (April 2005).

The UNAVCO software TEQC (Translate, Edit and Quality Check) was used to characterise the environment at each of the four stations. MP1 and MP2 code multipath proxy values (Estey and Meertens 1999) were extracted on the L1 and L2 frequencies respectively from the observation and navigation files of all site stations over the whole data period. Table 2 shows the overall mean and root mean square (RMS) values of MP1 and MP2 for all four stations with  $5^\circ$  and  $15^\circ$  elevation mask angles. It is evident that both DRMN and DRMS stations sustain high multipath for very low elevation satellites only, whereas NEWC and SN02 suffers from high multipath over much or all of the sky. For SN02, we suggest that this multipath is due to the high wall close to this station (Fig. 1).

Another dataset was collected in December 2005, 8 months after the first dataset, in order to test long-term variation in the “sidereal” lag. The common window of the secondary dataset runs from 12: 35: 05 (GPS time) on 13 December 2005 until 14: 16: 20 on 17 December 2005. The same types of receivers and antennas were used at the same stations.

### 4 Sidereal lag determination

Baselines DRMN-DRMS, DRMN-SN02 and DRMN-NEWC were processed, holding the coordinates of DRMN fixed. As can be seen from Table 1, the length of these baselines (up to a few hundred metres) is sufficiently short that all atmospheric, orbital and clock errors may be assumed to be removed by double differencing, and hence our results will depend on receiver noise and multipath error only.

We searched for the optimum lag (maximum autocorrelation among station coordinates), using window sizes from 30 s up to 10 h, centred on each hour. Window sizes of 30 s up to 30 min display large, apparently random, fluctuations in the optimal lag. Therefore, we show only the 0.5, 1, 2, 3, 4, 8 and 10 h window sizes. Figure 2 illustrates the optimum value of the lag as a function of time, for site SN02 (DRMS shows very similar behaviour). The 0.5- and 1-h window sizes again show high fluctuation from hour to hour, and thus the remaining five window sizes will be the ones focused upon.



**Fig. 1** Locations of the GPS Stations. **a** Drummond Stations (DRMS and DRMN); **b** Bedson Stations (SN02 and NEWC)

**Table 1** Data collection parameters of the first dataset (GPS week = 1,317)

| Station                       | DRMN                                | DRMS                   | SN02                                | NEWC                   |
|-------------------------------|-------------------------------------|------------------------|-------------------------------------|------------------------|
| Start time (GPS time)         | 04 April 2005 14:07:50 <sup>a</sup> | 04 April 2005 13:46:57 | 04 April 2005 11:16:35              | 04 April 2005 11:00:00 |
| End time (GPS time)           | 08 April 2005 14:47:50              | 08 April 2005 14:43:38 | 08 April 2005 14:25:05 <sup>a</sup> | 08 April 2005 17:59:59 |
| Receiver type                 | LEIGX1230                           | LEIGX1230              | LEIGX1230                           | ASHUZ-12               |
| Antenna type                  | LEIAX1202                           | LEIAX1202              | LEIAX1202                           | ASH700936-SNOW         |
| Pillar type                   | Concrete                            | Concrete               | Steel                               | Steel                  |
| Baseline length from DRMN (m) | –                                   | 11.27                  | 349.29                              | 339.59                 |

<sup>a</sup> Common start and end times of the processed dataset

**Table 2** Multipath parameters for all four stations for both 5° and 15° elevation masks

| Elevation mask | Multipath proxy | Value (m) | Station |      |      |      |
|----------------|-----------------|-----------|---------|------|------|------|
|                |                 |           | DRMN    | DRMS | SN02 | NEWC |
| 5°             | MP1             | Mean      | 0.30    | 0.29 | 0.27 | 0.35 |
|                |                 | RMS       | 0.65    | 0.68 | 0.59 | 0.48 |
|                | MP2             | Mean      | 0.41    | 0.39 | 0.36 | 0.34 |
|                |                 | RMS       | 1.01    | 0.94 | 0.78 | 0.47 |
| 15°            | MP1             | Mean      | 0.19    | 0.18 | 0.23 | 0.35 |
|                |                 | RMS       | 0.30    | 0.27 | 0.53 | 0.46 |
|                | MP2             | Mean      | 0.25    | 0.23 | 0.30 | 0.33 |
|                |                 | RMS       | 0.39    | 0.37 | 0.71 | 0.43 |

Increasing the window size, or in other words the number of considered epochs, decreases the apparent variability of the lag, which over the whole dataset tends to a steady value of around 86,154 s (23 h 55 m 54 s), i.e. not exactly sidereal, as previously reported by Choi et al. (2004) based on the mean satellite repeat period. The exception to this is the NEWC station, for which the lag does not completely stabilize even using a 10-h window. This could be attributed to its higher multipath environment, which causes frequent receiver loss of lock leading to data gaps, and thus increases the random noise.

Although we will concentrate on stations DRMS and SN02 in our discussion of optimum lag determination, we will later show that sidereal filtering at NEWC is highly effective. Sidereal lag studies were also performed

through correlating double-difference phase residuals at each epoch instead of 3D coordinates, and these yield the same results and conclusions.

An important question is whether the apparent variation in optimum geometry-repeat lag for the shorter window sizes in Fig. 2 is an artefact of the small sample size, or real and due to the variability in individual satellite ground track repeat times and its interaction with the local multipath reflectors (as suggested by Larson et al. 2006, <http://spot.colorado.edu/~kristine/publications.html>). More relevantly, we question whether such minor variations in the optimum lag have a significant impact on the performance of the sidereal filter, when using a double-difference processing method.

Figure 3 represents the variation of autocorrelation with lag at each epoch, for 2-h windows at station SN02.

**Fig. 2** Optimum geometry-repeat lag for different window sizes (SN02)

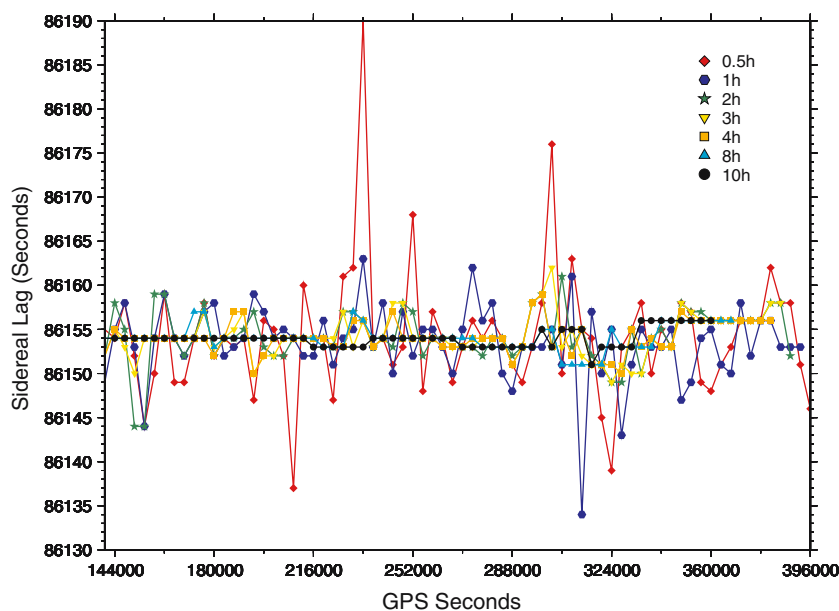


Figure 4 shows the same quantities for 10-hour windows. Figures 3 and 4 show that the maximum autocorrelation values fluctuate highly for the 2-h window, whereas they become more homogeneous for the 10-h window. The “striping” in Fig. 3 strongly suggests that there are times at which the sidereally repeating signal is weak or incoherent, perhaps due to a beneficial satellite geometry for which there is temporarily little or no multipath error.

To distinguish those epochs where the maximum autocorrelation is less well determined, as opposed to those where the autocorrelation is simply weaker, Fig. 5 shows the “sidereal” lags having an autocorrelation equal to or greater than 95, 97 and 99% of the maximum autocorrelation value at that epoch (for a 2-h window). The 10-h window optimum lag is overlaid in Fig. 5. It can be seen that the optimal 10-h lag lies nearly always within the 99% threshold, implying that the longer-term estimate of geometry-repeat lag is never significantly worse than the short-term one.

Conversely, Fig. 6 represents the same threshold limits but for the 10-h window, with the 2-h window optimum lag overlaid. Although the 2-h lag shows greater fluctuation when compared to the 10-h, these fluctuations are always within the 97% threshold of the latter. In other words, the short- and long-window lag values are consistent, and use of the longer-window lag value (or even a constant value) should not appreciably worsen the filtering.

We repeated this analysis using our second dataset collected 8 months after the first, during which time the satellite constellation had changed slightly, and again found that a constant lag of 86,154 s gave an autocorrelation satisfactorily close to that of the optimal lag. This

essentially confirms the analysis of Choi et al. (2004), which was based on mean satellite orbit repeat period rather than the actual periodicity of coordinate or phase residuals. However, we additionally see here that variations within  $\pm 5$  s of the optimal lag do not appreciably worsen the autocorrelation. As an aside, we note that the limits of acceptable autocorrelation for SN02 are wider than for DRMS, due to the noisier environment of SN02.

## 5 Application of the sidereal filter

We form a filter either using the first day (case *Day 1*), two days (case *Day 1,2*) or from the first three days of data (case *Day 1,2,3*) using the optimum geometry-repeat lag and adopting two different stacking methodologies. The first is to stack the output coordinate residuals directly (coordinate stacking), and then to subtract these residuals from the appropriate epoch on the fourth day to give our final filtered coordinates.

The second method, carrier-phase residual stacking (phase stacking), includes two main steps. Firstly, we fix the coordinates of the unknown station and process the data to yield biased double-difference carrier-phase residuals for all independent satellite pairings at each frequency, which we then stack. Secondly, we re-process the data to give final filtered coordinates, having subtracted the stacked phase residuals from the corresponding L1 and L2 double-difference phase observables on the fourth day. Figure 7 shows the coordinate time series of NEWC station in east (E), north (N) and

**Fig. 3** Two-hour window autocorrelation (SN02)

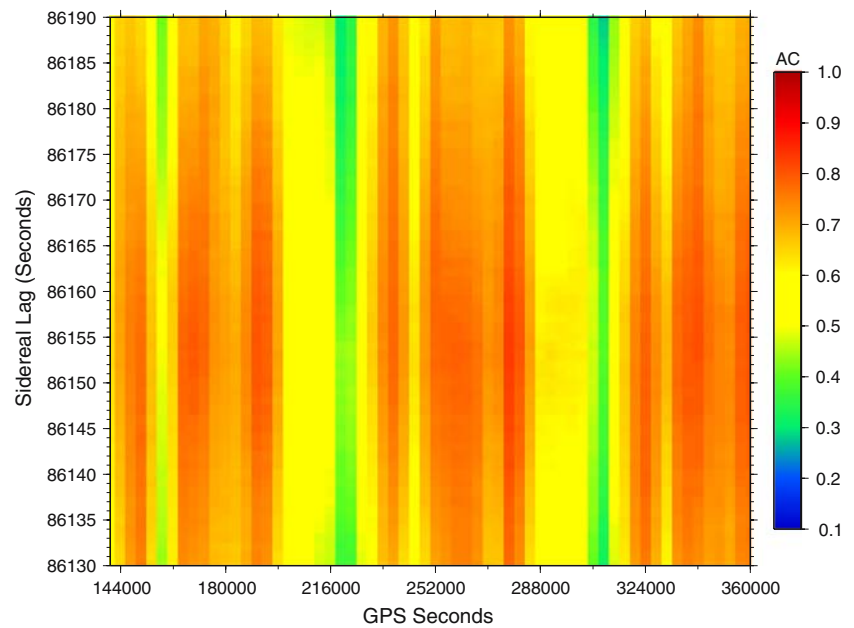
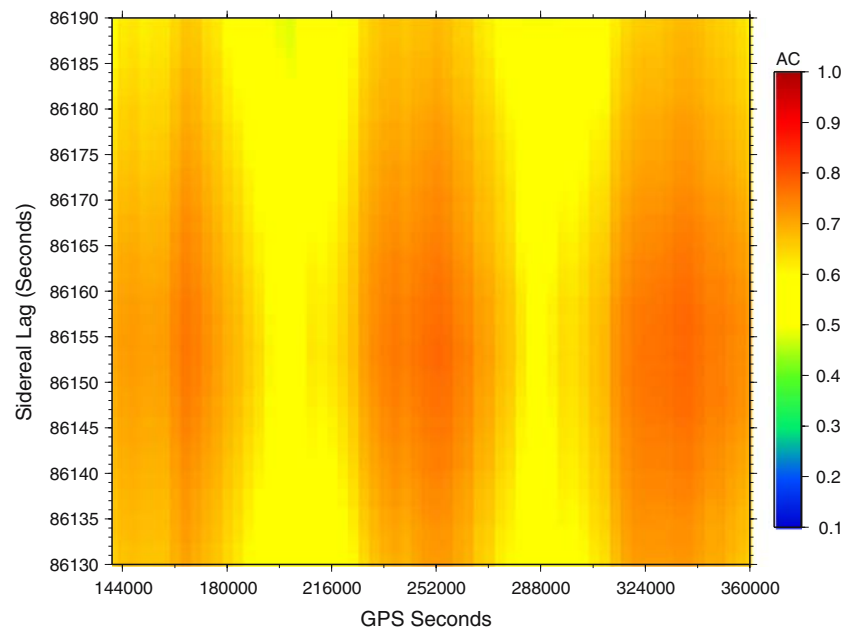


**Fig. 4** Ten-hour window autocorrelation (SN02)



up (U) directions for the unfiltered case and for each of these filtering methods.

Since the factor of improvement (the ratio of coordinate standard deviation before and after filtering) is virtually the same for E, N and U components, the change in 3D coordinate standard deviation will reflect more clearly and simply the effect of the applied filter. Table 3 gives the 3D coordinate standard deviation over the entire fourth day for both methodologies for all three cases. This shows the overall improvement in the precision after the filter, which is greatest when stacking three

days together. Accordingly we adopt the three-day filter hereafter.

Figures 8 and 9 show the 3D hourly standard deviation for coordinate and phase residual stacking respectively. Both methods achieve a clear improvement in precision, but the coordinate filtering method is slightly superior in this regard. After sidereal filtering, the standard deviation becomes significantly smaller at the 95% confidence level in almost every hourly window, and also more consistent and homogeneous. The filtered standard deviation decreases to a roughly similar value

**Fig. 5** Two-hour window threshold (SN02). Values are expressed as a percentage of the maximum autocorrelation. The *solid line* shows the optimal lag for a 10-h window

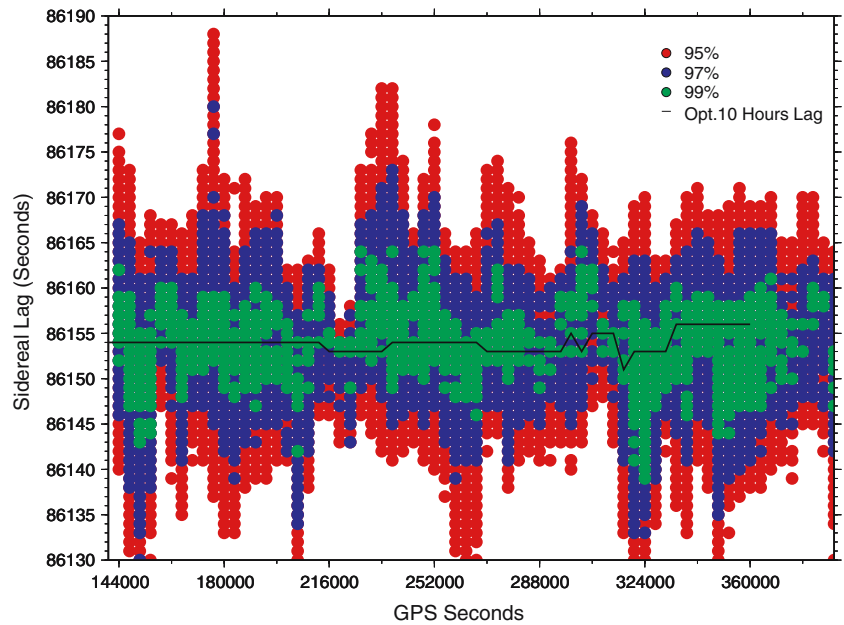
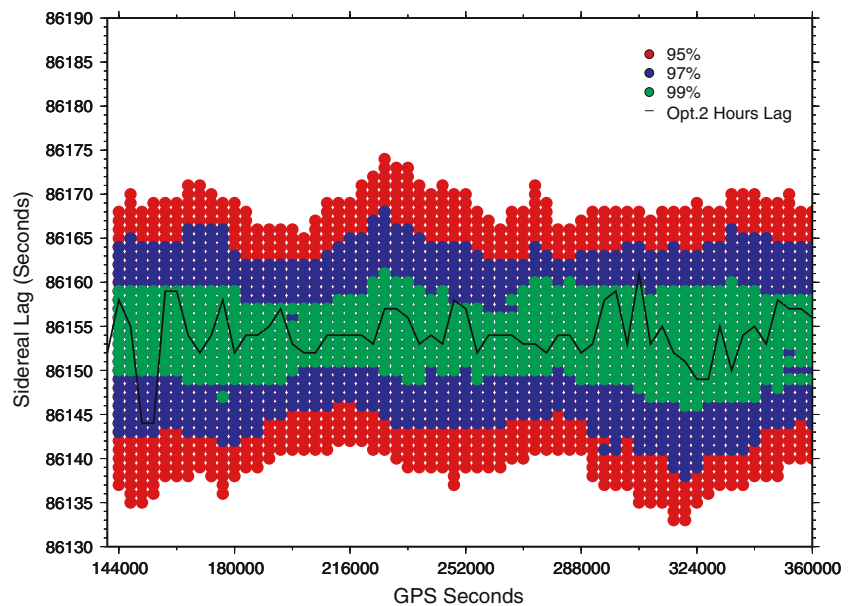


**Fig. 6** Ten-hour window threshold (SN02). Values are expressed as a percentage of the maximum autocorrelation. The *solid line* shows the optimal lag for a 2-h window



for all three stations, regardless of the unfiltered standard deviation or multipath environment surrounding each station, which confirms the efficiency of the sidereal filtering. The good hour-to-hour consistency of the precision of the filtered coordinates, when using a constant lag, suggests that short-term variations in the optimum lag are relatively unimportant for “sidereal” filtering when using a double-differencing processing strategy.

Although both methods yield similar precision, the phase filtering method is clearly superior in the CPU time required. In the case of coordinate stacking, GASP is run once regularly to output raw coordinates for each

of the three “reference” days, followed by stacking of the coordinate residuals and application of the filter to the fourth day. Conversely, in the case of phase residual stacking, GASP must be run firstly for the three “reference” days with fixed coordinates to give residuals, followed by stacking of the phase residuals, and secondly, to process the fourth day with the stacked residuals applied.

Because GASP performs an ambiguity search at each epoch of regular processing but does not require this for fixed baselines, these coordinate-fixed runs are much faster than a normal run (about 57 s compared with 444 s for a 24-h dataset). Likewise, processing of the fourth

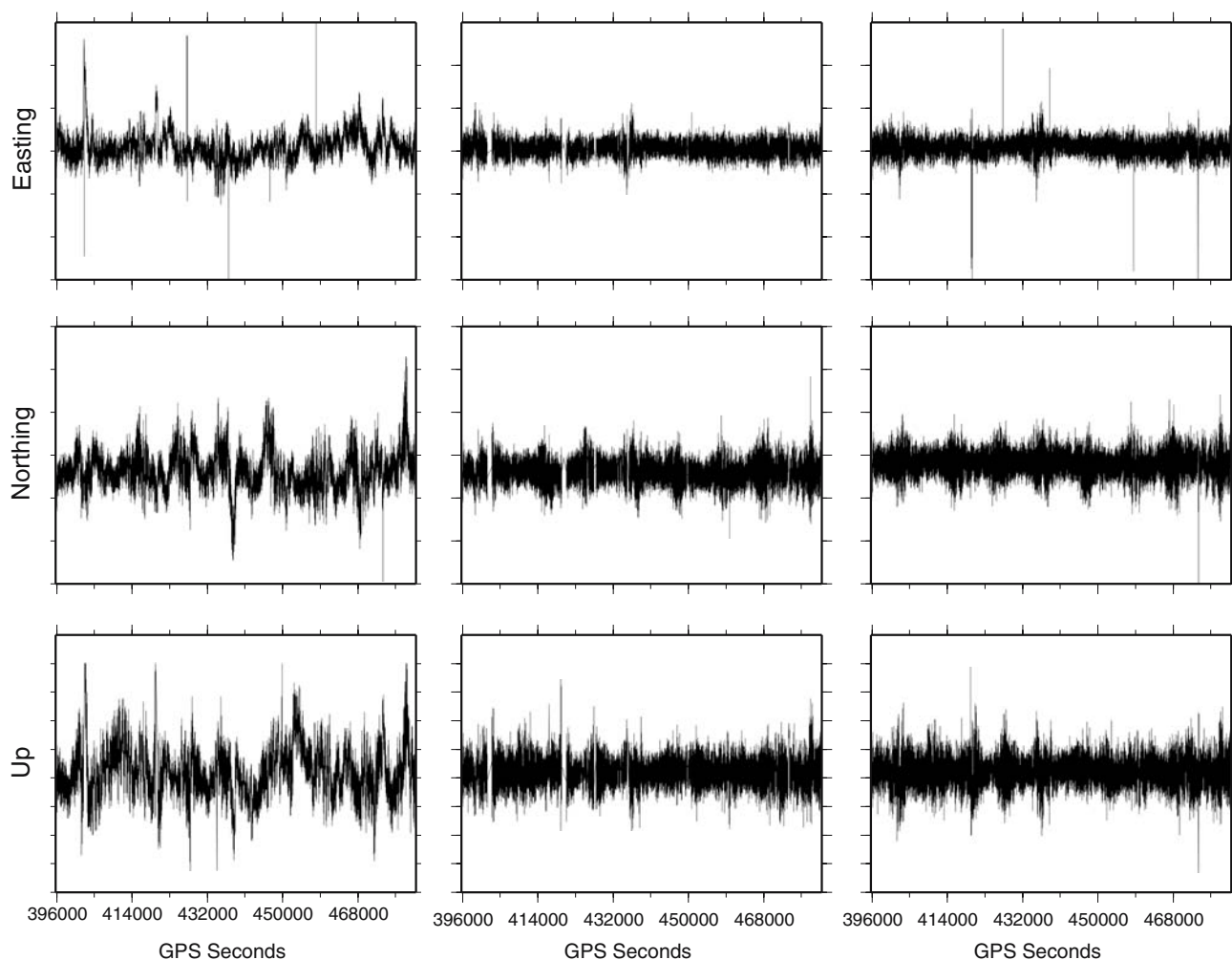


**Fig. 7** NEWC station E, N and U coordinate time-series. Note that the coordinate scale of E and N differ from that of U by a factor of 1.5 (Y-axis tick marks are at 1 cm intervals); (left) unfiltered; (middle) coordinate filter; (right) phase filter

**Table 3** 3D coordinate standard deviation (SD) over a 24-h period (stacking either one, two or three days to form the filter)

| Station | 3D SD (mm)/Case |                   |          |            |              |          |            |
|---------|-----------------|-------------------|----------|------------|--------------|----------|------------|
|         | Unfiltered      | Coordinate filter |          |            | Phase filter |          |            |
|         |                 | Day 1             | Days 1,2 | Days 1,2,3 | Day 1        | Days 1,2 | Days 1,2,3 |
| SN02    | 6.9             | 6.2               | 5.3      | 4.9        | 6.4          | 5.6      | 5.1        |
| DRMS    | 6.5             | 5.6               | 4.9      | 4.6        | 5.8          | 5.1      | 4.8        |
| NEWC    | 9.5             | 6.3               | 5.3      | 4.9        | 6.7          | 5.6      | 5.1        |

day with filtered phase observations increases the speed of the ambiguity search procedure because acceptable values are found within a smaller search volume. Table 4 indicates the time required for each phase of both stacking methods until reaching final filtered coordinates.

It can also be seen from Table 4 that the required processing time for the NEWC station using regular processing or coordinate stacking is significantly higher due to the high multipath environment of this station,

which affects the ambiguity-searching performance of the GASP program. Conversely, in the case of phase residual stacking, the processing time for all three stations is almost the same, which again confirms the usefulness of sidereal phase filtering to reduce the ambiguity search time, even in high multipath environment.

Although an independent epoch-by-epoch algorithm such as GASP represents an extreme case of this reduction in computation time, the phase residual stacking

**Fig. 8** Hourly 3D coordinate standard deviation, based on coordinate stacking. *Solid lines* show filtered values, *dashed* are for unfiltered

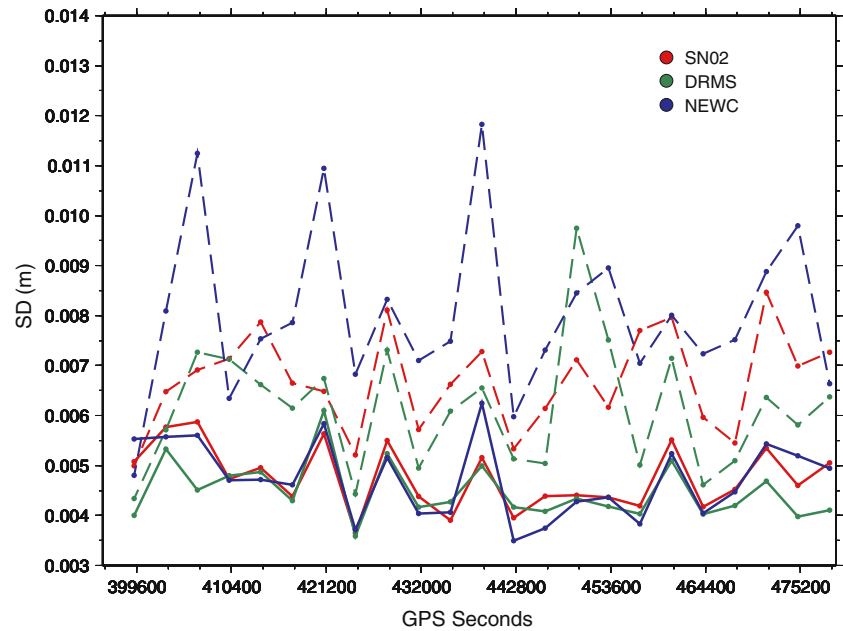
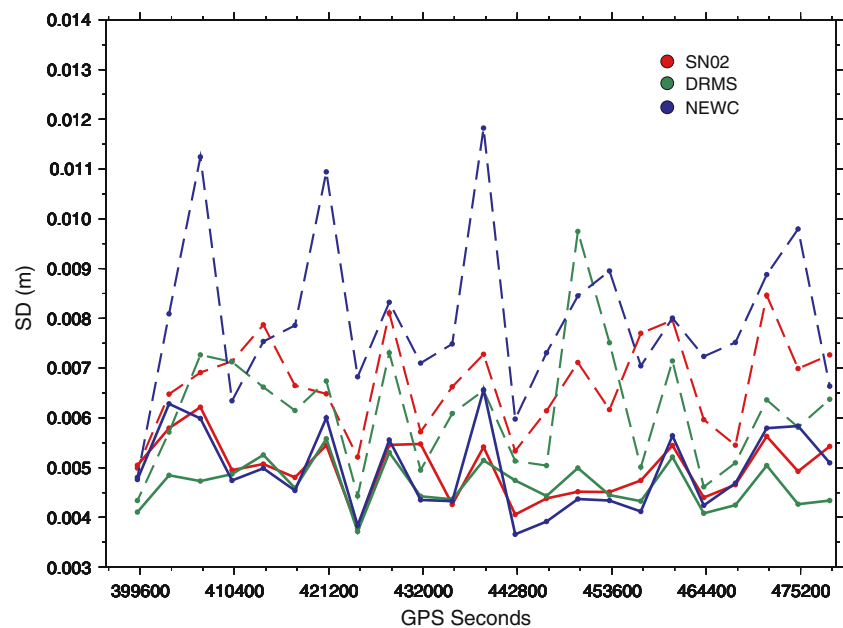


**Fig. 9** Hourly 3D coordinate standard deviation, based on phase residual stacking. *Solid lines* show filtered values, *dashed* are for unfiltered



approach will reduce processing effort to some extent in all non-epoch-by-epoch methods. This is particularly true in high multipath and reduced-sky-visibility environments, where frequent losses of lock can be expected to lead to re-estimation of ambiguity parameters.

To verify the previous results, the second dataset was processed in the same manner, but only two window sizes for “sidereal” lag determination (2 and 10 h) were investigated. This confirmed the results obtained from the first dataset regarding the optimum geometry-repeat

lag, effect of window size and efficiency of sidereal filtering for minimizing the multipath error.

Table 5 is formed in a similar manner to Table 3, but only for the case of stacking three days together and the unfiltered case. Table 5 also shows sidereal filter results using the nominal lag (86, 164 s), and again confirms the improvement obtained using the modified near-sidereal lag compared with the nominal sidereal lag. However, the difference between using the optimal and nominal lags is small compared with the unfiltered case, again

**Table 4** Processing time for each step of both stacking methods, on a Linux workstation

| Method            | Procedure                                 | SN02        | DRMS        | NEWC        |
|-------------------|-------------------------------------------|-------------|-------------|-------------|
| Coordinate filter | Three Days processing                     | 22 min 12 s | 19 min 54 s | 42 min 24 s |
|                   | Processing 4th day and filter application | 7 min 32 s  | 6 min 40 s  | 14 min 33 s |
|                   | Total time                                | 29 min 44 s | 26 min 34 s | 56 min 57 s |
| Phase filter      | Three Days processing                     | 2 min 51 s  | 2 min 59 s  | 2 min 36 s  |
|                   | Processing 4th day and filter application | 7 min 08 s  | 7 min 08 s  | 6 min 26 s  |
|                   | Total time                                | 09 min 59 s | 10 min 07 s | 09 min 02 s |

**Table 5** 3D coordinate standard deviation over a 24-h period, secondary dataset (3-day filter stacking)

| Station | 3D SD (mm)/lag/methodology |                   |              |                   |              |
|---------|----------------------------|-------------------|--------------|-------------------|--------------|
|         | Unfiltered                 | 23 h 55 m 54 s    |              | 23 h 56 m 04 s    |              |
|         |                            | Coordinate filter | Phase filter | Coordinate filter | Phase filter |
| SN02    | 7.4                        | 5.8               | 6.1          | 6.0               | 6.3          |
| DRMS    | 6.7                        | 5.4               | 5.8          | 5.7               | 6.1          |
| NEWC    | 9.7                        | 6.6               | 7.0          | 6.9               | 7.4          |

showing that minor variations in the adopted lag do not impact greatly on the final coordinates.

## 6 Conclusions and recommendations

It is generally clear that as the number of epochs used in the determination of the sidereal lag increases, the optimum geometry-repeat lag tends to a more consistent, steady and uniform value throughout the whole dataset. A long window size (8–12 h) is recommended for the determination of the optimum “sidereal” lag, although a usable value can be obtained from a shorter window; e.g., a 2-h window will always have an autocorrelation with at least 97% of the optimal longer-term value, despite showing greater fluctuation. Short-term variations in the optimum lag appear to have little effect on the final filtered coordinate precision, at least for double-difference processing. This factor may, however, be relevant to undifferenced processing strategies.

We find that the optimum geometry-repeat lag is 86, 154 s (23 h 55 m 54 s), i.e., 10 s less than the nominal sidereal lag. This independently confirms the results obtained by Choi et al. (2004), with very slight differences mainly because the studies of Choi et al. (2004) were based on orbital information, taking minimum 15° elevation angle and applying box filtering for noise reduction, whereas this study was based on the autocorrelation of coordinate and phase residuals, taking a minimum 5° elevation angle without applying any noise reduction filter. Our lag value was tested using two datasets with 8-month time difference, and is not significantly altered over this interval.

The use of sidereal filtering minimizes the multipath effect on GPS data and accordingly improves the overall precision of the final station coordinates. Statistically, coordinate stacking gives slightly better precision than phase residual stacking, but with similar hour-to-hour consistency of results. However, coordinate stacking requires significantly longer processing time, especially if an epoch-by-epoch ambiguity searching algorithm is used, and this may outweigh the relatively small difference in final coordinate precision.

**Acknowledgments** We thank Kristine Larson and an anonymous reviewer for their constructive criticism, which did much to improve this manuscript. We also thank Martin Robertson (Newcastle University) for technical support, and Mark Greaves and colleagues (Ordnance Survey) for timely provision of the 1 s data for NEWC. A. Ragheb is partially supported by an Overseas Research Scholarship funded by Universities UK.

## References

- Al-Haifi Y (1996) Short range GPS single epoch ambiguity resolution. PhD thesis, Department of Surveying, University of Newcastle upon Tyne
- Axelrad P, Comp CJ, MacDoran PF (1996) SNR-based multipath error correction for GPS differential phase. *IEEE Trans Aerosp Electron Syst* 32(2):650–660
- Choi K, Bilich A, Larson K, Axelrad P (2004) Modified sidereal filtering: implications for high-rate GPS positioning. *Geophys Res Lett* 31, L22608. Doi 10.1029/2004GL021621
- Corbett S (1994) GPS single epoch ambiguity resolution for airborne positioning and orientation. PhD thesis, Department of Surveying, University of Newcastle upon Tyne
- Estey L, Meertens C (1999) TEQC: The multi-purpose toolkit for GPS/GLONASS data. *GPS Solut* 3(1):42–49

- Filippov V, Tatarnicov D, Ashjaee J, Astakhov A, Sutiagin I (1999) The first Dual-depth Dual-frequency choke ring. In: Proceedings of the 12th Technical meeting of the Satellite Division of the Institute of Navigation, ION GPS-99, Nashville Convention Centre, Nashville
- Genrich J, Bock Y (1992) Rapid resolution of crustal motion at short ranges with the global positioning system. *Geophys Res Lett* 19:3261–3269
- Larson K, Bilich A, Axelrad P (2006) Improving the precision of high-rate GPS. *J Geophys Res* (submitted)
- Lau L, Mok E (1999) Improvement of GPS Relative Positioning accuracy by using SNR. *J Surveying Eng-ASCE* 125(4):185–202
- Leick A (2004) *GPS Satellite Surveying*. Wiley, New York
- Neilan R, Zumberge J, Beutler G, Kouba J (1997) The International GPS Service: A Global Resource for GPS Applications and Research. In: Proceedings of 10th Technical meeting of the Satellite Division of the Institute of Navigation, ION GPS-97, Kansas City Convention Centre, Kansas City
- Nikolaïdis R, Bock Y, de Jonge P, Shearer P, Agnew D, Van Domselaar M (2001) Seismic wave observations with the global positioning system. *Geophys Res Lett* 28(B10):21897–21916
- Penna N, Stewart M (2003) Aliased tidal signatures in continuous GPS height time series. *Geophys Res Lett* 30(23):2184. Doi 10.1029/2003GL018828
- Satirapod C, Rizos C (2005) Multipath mitigation by wavelet analysis for GPS base station applications. *Surv Rev* 38(295):2–10
- Van Dierendonck AJ, Braasch MS (1997) Evaluation of GNSS receiver correlation processing techniques for multipath and noise mitigation. In: Proceedings of the National Technical meeting “Navigation and Positioning in the Information Age”, Loews Santa Monica Beach Hotel, Santa Monica
- Zheng D, Zhong P, Ding X, Chen W (2005) Filtering GPS time-series using a Vondrak filter and cross-validation. *J Geod* 79(6–7):363–369